Published in final edited form as:
*Circ Res*. 2013 January 4; 112(1): 57–65. doi:10.1161/CIRCRESAHA.112.274456.

# Acute L-CPT1 Overexpression Recapitulates Reduced Palmitate Oxidation of Cardiac Hypertrophy

**E. Douglas Lewandowski**[1], **Susan K. Fischer**[1], **Matthew Fasano**[1], **Natasha H. Banke**[1], **Lori A. Walker**[2], **Alda Huqi**[3], **Xuerong Wang**[1], **Gary D. Lopaschuk**[3], and **J. Michael O'Donnell**[1]

[1]Center for Cardiovascular Research, University of Illinois at Chicago College of Medicine, Chicago IL 60612

[2]Division of Cardiology, Department of Medicine, University of Colorado School of Medicine, Aurora, CO 80045

[3]Mazankowski Alberta Heart Institute, Departments of Pediatrics and Pharmacology, University of Alberta, Edmonton, Alberta, CA.

## Abstract

**Rationale—**Muscle carnitine palmitoyltransferase I (M-CPT1) is predominant in heart, but the liver isoform (L-CPT1) is elevated in hearts with low long chain fatty acid (LCFA) oxidation, such as fetal and hypertrophied hearts.

**Objective—**This work examined the effect of acute L-CPT1 expression has on the regulation of palmitate oxidation and energy metabolism in intact functioning rat hearts for comparison to findings in hypertrophied hearts.

**Methods and Results—**L-CPT1 was expressed *in vivo* in rat hearts by coronary perfusion of Adv.cmv.L-CPT1 (L-CPT1, n=15) versus PBS infusion (PBS, n=7) or empty virus (EMPTY, n=5). L-CPT1 was elevated 5-fold at 72 hours after Adv.cmv.L-CPT1 infusion ($P<0.05$), but M-CPT1 was unaffected. Despite similar tricarboxylic acid cycle rates, palmitate oxidation rates were reduced with L-CPT1 (1.12±0.29 micromole/min/g dw, mean ± SE) vs PBS (1.6±0.34). Acetyl CoA production from palmitate was reduced with L-CPT1 (69%±0.02, $P<0.05$; PBS= 79%±0.01, Empty=81%±0.02), similar to what occurs in hypertrophied hearts and with no difference in malonyl CoA content. Glucose oxidation was elevated with L-CPT1 (by 60%). Surprisingly, L-CPT1 hearts contained elevated atrial natriuretic peptide, indicating induction of hypertrophic signaling.

**Conclusions—**The results link L-CPT1 expression to reduced palmitate oxidation in a non-diseased, adult heart, recapitulating the phenotype of reduced LCFA oxidation in cardiac hypertrophy. The implications are that L-CPT1 expression induces metabolic remodeling hypertrophic signaling, and that regulatory factors beyond malonyl-CoA in the heart regulate LCFA oxidation via L-CPT1.

**Address correspondence to:** Dr. E. Douglas Lewandowski Director, Center for Cardiovascular Research UIC College of Medicine 909 South Wolcott Avenue MC 801 Chicago, IL 60612 Tel: 312-413-7261 Fax: 312-996-2870 dougl@uic.edu.

**DISCLOSURES** Gary Lopaschuk is a major shareholder of Metabolic Modulators Research Ltd.

**Keywords**

Palmitoyltransferase I; long chain fatty acids; beta-oxidation; mitochondria; hypertrophy

## INTRODUCTION

The current study examines the consequences of mimicking the isoform shift in the carnitine palmitoyltransferase I (CPT1) enzyme that occurs in pathologically hypertrophied myocardium, on fatty acid oxidation in the otherwise normal, intact beating rat heart (1-4). CPT1 is responsible for the rate-limiting component of long chain fatty acid (LCFA) oxidation by cardiac mitochondria. We report here the metabolic shifts induced by acute overexpression of the liver isoform of CPT1, that has been observed to be elevated in cardiomyocytes developing pathological hypertrophy. Reductions in LCFA oxidation are well recognized to occur in hypertrophied myocardium, and are associated with changes in the expression of associated metabolic enzymes (1-6). These changes influence the rate-limiting step of LCFA oxidation that occurs in the outer mitochondrial membrane at the enzyme, CPT1. Along with reporting reduced rates of long chain fatty acid oxidation in cardiac hypertrophy, our laboratory first demonstrated a shift in CPT1 isoform distribution toward L-CPT1, by reporting elevated L-CTP1 protein content in hypertrophied rat hearts (3). The present study examines the direct influence of similarly elevated expression of L-CPT1 on the oxidative metabolism of the otherwise normal, nonpathological rat heart due to acute, targeted delivery and cardiac expression of the L-CPT1 gene.

The mitochondrial membrane is impermeable to LCFA's which are oxidized via β-oxidation and the tricarboxylic acid (TCA) cycle in the inner matrix. CPT1 serves as a translocase for fatty acyl esters, by spanning the outer mitochondrial membrane and catalyzing acyl group transfer from coenzyme A to carnitine (7). There are two structural genes that encode CPT1, one for the L (liver) or *a* isoform of the enzyme, and one for the M (muscle) or *b* isoform (1,2,7,8). These CPT1 isoforms are differentially expressed among tissues that utilize LCFA's as a fuel, and both isoforms are co-expressed in heart muscle. In adult heart muscle, M-CPT1 is the predominantly expressed isoform, with limited activity from L-CPT1 (1-3,9-11). However, until recently the actual content of L-CPT1 which is elevated in the hypertrophied heart, as opposed to transcript levels from myocardium or analysis activity in cultured neonatal cardiomyocytes, was not known (2,3,12).

The L and M isoforms of CPT1 have different kinetic properties, with L-CPT1 being the less sensitive to malonyl CoA inhibition and displaying a higher affinity for carnitine (7,9). Yet, LCFA oxidation is lower in hearts with elevated L-CPT1 content (i.e. hypertrophied adult hearts and neonatal hearts) than in normal adult hearts displaying minimal L-CPT1 activity (1-6,9,11,13,14). Elevated L-CPT1 levels in cardiomyocytes, in culture, has been explained as an potential adaptive response, based on the teleological argument that L-CPT1 expression serves the functional outcome of maintaining fatty acid oxidation, albeit reduced (2). Indeed, the link between increased L-CPT1 and reduced palmitate oxidation is also consistent with a reversion to fetal isoform expression of metabolic enzymes and reduced LCFA oxidation rates under conditions of limited carnitine availability in fetal and neonatal hearts (1,2,9,10,13). These seemingly incongruent findings between L-CPT1 expression and LCFA oxidation may also suggest a multifactorial level of regulation of LCFA oxidation to produce the observed metabolic phenotypes. However, no previous work has examined the direct influence of isoform shifts in CPT1 on LCFA oxidation rates in the intact, adult heart in the absence of disease.

Therefore, this study examined what effect acute overexpression of L-CPT1 has on energy metabolism in the adult rat heart, following in vivo delivery and expression of exogenous L-CPT1 gene. The utility of the acute overexpression model enabled an examination of metabolic adaptations to L-CPT1 expression and the direct influence of L-CPT1 expression on LCFA oxidation, in the absence of developmental adaptations due to chronic overexpression. The aims of this study were to: 1) examine the effects of increased L-CPT1 content in the otherwise normal, adult rat heart on rates of palmitate oxidation, 2) determine the effects of increased L-CPT1 expression on M-CPT1 expression in adult rat hearts, 3) compare the fraction of palmitate contributing to acetyl CoA formation in the TCA in hearts with acute overexpression of L-CPT1 compared to both sham infected controls with normal CPT1 isoform distributions and to hearts with pressure overload hypertrophy, and 4) examine the potential responses in proteins indicative of the hypertrophic stimulus in hearts with acute overexpression of L-CPT1, sham infected control hearts, and hypertrophied hearts. The outcome offers new insight into the complex integration of enzyme expression and activities within metabolic networks that are linked to changes in pathophysiological state.

## MATERIALS AND METHODS

### Heart models

All protocols and procedures involving animals were approved by the Animal Care Policies and Procedures Committee at the University of Illinois in Chicago (Institutional Animal Care and Use Committee accredited), and animals were maintained in accordance with the *Guide for the Care and Use of laboratory Animals* published by the US National Institutes of Health (NIH Publication No. 85-23, revised 1996).

Adult rats (male, Sprague Dawley, 400-450 gm) were anesthetized (i.p. pentobarbital, 50 mg/kg, 1% isoflurane inhalation) and *in vivo* intracoronary perfusion of the heart was performed with either adenovirus carrying cDNA for the rat liver isoform of the carnitine palmitoyltransferase I (Adv.cmv.L-CPT1) at $8\times10^{12}$ viral particles/ml PBS (0.4 ml), adenovirus carrying scrambled cDNA (empty) at $8\times10^{12}$ vp/ml as a viral delivery control group, or 0.4 ml PBS as a sham control (15,16) (See Supplemental Material). The adenovirus expresses the liver isoform of the carnitine palmitoyltransferase I gene ($10^{12}$ viral particles/ml PBS) under a CMV promoter. Use of the viral vector did not influence L-CPT1 expression in the absence of code for L-CPT1 (See Online Figure II).

In other groups, anesthetized rats received transverse aortic constriction (TAC) to produce pressure overload or sham surgery, as previously described (3,6,16). TAC produces concentric cardiac hypertrophy and increased heart to body weight ratio within 10 weeks post-surgery. At 10 weeks post-surgery, experiments were performed on isolated hearts from these animals.

Hearts were excised from anesthetized rats (pentabarbital, 50 mg/kg, i.p.) at 72 hours following intracoronary perfusion or 10 weeks following TAC. Excised hearts were either immediately perfused or frozen for assays.

### C enrichment protocols for metabolic flux measurements[13]

Rates of LCFA oxidation and/or the fraction of palmitate contributing to acetyl-CoA synthesis for the TCA cycle were determined in isolated, perfused rat hearts excised from rats that were anesthetized (see above) and heparinized (500 U/100g i.p.); L-CPT1, n = 15; PBS sham, n = 7. Similarly, hearts were perfused from rats subjected to TAC (n = 14) or sham operation (n = 11). Isolated hearts were perfused in a retrograde fashion at 37°C, as previously described, with modified Krebs-Henseleit buffer (116 mM NaCl, 4 mM KCl, 1.5

mM $CaCl_2$, 1.2 mM $MgSO_4$ and 1.2 mM $NaH_2PO_4$, equilibrated with 95% $O_2$/5% $CO_2$ with 0.4 mM unlabeled palmitate/albumin complex (3:1 molar ratio) and 5 mM glucose) (3,6,16). A water-filled latex balloon in the left ventricle was set to a diastolic pressure of 5 mmHg and provided hemodynamic recordings (Powerlab, AD Instruments, Colorado Springs, CO). Left ventricular developed pressure and heart rate were continuously recorded. After each perfusion, hearts were frozen for biochemical analyses. For palmitate oxidation, isolated hearts were initially supplied buffer containing unlabeled palmitate/albumin and glucose for 10 minutes to ensure metabolic equilibrium and for collection of background $^{13}$C-NMR signals of naturally abundant $^{13}$C (1.1%). At the start of each enrichment protocol, the perfusate was switched to buffer (1 liter) containing [2,4,6,8,10,12,14,16-$^{13}C_8$] palmitate (0.4 mM) (Isotec, Inc., Miamisburg, OH) plus unlabeled glucose (5 mM). Perfusion with $^{13}$C-enriched media continued for 40 minutes.

For metabolic flux measurements, a subset of these hearts (L-CPT1, n = 10; PBS Sham, n = 5) were situated in a 20 mm NMR probe within a vertical 89 mm bore, 9.4 T magnet. $^{31}$P and $^{13}$C NMR (2 min each) measurements were acquired as described elsewhere (3,17). Energetic state was determined by $^{31}$P NMR detection of phosphocreatine and ATP content (3).

Metabolic flux in the intact beating heart was determined during $^{13}$C palmitate delivery to the intact rat heart *ex vivo* using well described methods for kinetic analysis of the progressive $^{13}$C enrichment of glutamate, via NMR spectroscopy (3,17) (see Supplemental Material). Kinetic analysis provided: 1) TCA cycle flux, 2) the interconversion rate between cytosolic glutamate and mitochondrial α-ketoglutarate via the oxoglutarate-malate carrier, and 3) $^{13}$C palmitate entry into the mitochondria as an index of CPT1 flux.

Hearts from additional experimental groups of Adv.cmv.L-CPT1-infected rats (n = 7) and PBS infused control rats (n = 5) were perfused with unenriched palmitate (0.4 mM) plus [1,6-$^{13}C_2$] glucose (5 mM) to assess potential differences in glucose oxidation.

## Tissue biochemistry

Assays for glutamate, aspartate, citrate malate, and α-ketoglutarate were determined spectrophotometrically and fluorometrically (17-21). Triacylglycerol (TAG) was determined by colorimetry of processed lipid extracts (Wako Pure Chemical Industries) (6). Malonyl-CoA was assayed by high-pressure liquid chromatography with UV detection (22,23).

The percent of labeled acetyl CoA entering the TCA cycle was determined from *in vitro* $^{13}$C NMR spectra (6,24). Enrichment of glutamate from [1,6-$^{13}C_2$] glucose was determined via $^{13}$C NMR of *in vitro* tissue extracts and the relative contributions of $^{13}$C enriched glucose and the unlabeled ($^{12}$C) endogenous pool of glycogen determined via $^{1}$H NMR of alanine enrichment (3,25).

For Western blot assay of CPT1, hearts excised from both PBS shams (n = 7) and L-CPT1 heart (n = 3) were perfused with ice cold MSE media containing protease inhibitors. The left ventricle was minced and homogenized in 1 ml of ice-cold MSE media and centrifuged at 12000 × rpm for 15 minutes. Rat liver was used as a positive control for L-CPT1 content. Total homogenate protein concentration was determined from a standard curve (Bradford assay) and equivalent samples (80-100 microgram protein) were dissolved in Laemmli buffer, then loaded and separated on a 7.5 % NuPAGE Bis-Tris gel. Gel proteins were subsequently transferred onto a nitrocellulose membrane. Western blots were performed according to the standard techniques using human heart (HH) M-CPT1 Ab and rat liver (RL) L-CPT1 Ab (3). Semi-quantitative densitometric analysis was performed using the Bio-Rad Universal Hood and Quantity One software. Message level for ANP expression was

determined after total RNA isolation by single extraction with an acid guanidinium thiocyanate-phenol-chloroform mixture (3,26).

Myocardial contents of acetyl CoA carboxylase 2 (ACC2) and phosphorylated ACC2 (P-ACC2, Ser 218) and malonyl CoA decarboxylase (MCD) were determined in the available myocardial tissue from L-CPT1 hearts (n = 13), PBS shams (n = 7), hypertrophied hearts (n = 4), and Sham operated hearts (n = 4). ACC2 and P-ACC2 were probed with corresponding antibodies as previously described (Upstate Cell Signaling Technologies USA) (27). MCD was immunoblotted with an antiMCD antibody (H2-40 antibody, prepared in-house) as detailed elsewhere (27).

### Statistical analysis

Inter-group statistics were analyzed using Student t-test for comparison of two mean values and one-way ANOVA analysis with the Tukey post-test for comparison of multiple groups means. Statistical significance was established at 5% probability ($P < 0.05$). All reported values are reported as averages ± SEM.

## RESULTS

### Response of CPT1 expression to exogenous L-CPT1 gene delivery

Following adenoviral delivery of the exogenous gene for rat L-CPT1 to the in vivo heart, the level of L-CPT1 protein was increased in adv.cmv.L-CPT1 infected hearts 5-fold over L-CPT1 content in control hearts receiving sham infusions of phosphate buffered saline (PBS), as displayed in Figure 1 (15,16). The content of M-CPT1 remained unchanged in the presence of elevated L-CPT1 (Figure 1). The level of L-CPT1 overexpression that was achieved was similar to the approximate 4-5 fold increase in L-CPT1 protein that was previously reported for hypertrophied rats (3).

### Oxidative rates and metabolism of palmitate in L-CPT1 expressing, adult rat hearts

The functional workloads, as assessed by rate-pressure-products generated by the perfused hearts, were similar (Figure 2), and thus the metabolic demand imposed by cardiac workload was the same in the sham and L-CPT1 expressing groups. Consequently, mitochondrial oxidative rates, as assessed by TCA cycle flux from dynamic-mode $^{13}C$ NMR of the beating hearts (Figure 3A) were also similar with either L-CPT1 (12.3 ± 1.0, μmole/min/g dw, mean ± SE) expression or PBS infusion (15.0 ± 1.5).

However, despite similar rates of flux within the TCA cycle, the rate of palmitate oxidation in the intact hearts was unexpectedly reduced in hearts expressing L-CPT1 in comparison to PBS infused controls. L-CPT1 expression produced a 30% reduction in the rate of palmitate oxidation compared hearts receiving PBS (Figure 3B), indicating lower rates of flux through CPT1 in the hearts with elevated L-CPT1 (3).

Palmitate oxidation was reduced similarly in hypertrophied hearts and hearts with increased L-CPT1 content, as shown by reductions in the formation of acetyl CoA entering the TCA cycle from β-oxidation of palmitate (Figure 4). Figure 4A displays representative *in vitro* $^{13}C$ NMR spectra of the 4-carbon glutamate resonance in acid extracts of myocardium from an L-CPT1 expressing heart (right) and a PBS infused control (left), displaying the visual and quantitative differences between multiplet structure of the resonance signals that resulted due to differences in the oxidation of [2,4,6,8,10,12,14,16-$^{13}C_8$] palmitate (6). From static measures of $^{13}C$ NMR spectra from myocardial extracts (Figure 4A), the fraction of exogenous $^{13}C$ enriched palmitate contributing to acetyl CoA production within the mitochondria of isolated perfused hearts was reduced by 12% in myocardium that

overexpressed L-CPT1 (Figure 4B) in comparison to PBS controls. This drop mimicked the same 12% reduction observed in hypertrophy hearts versus sham operated hearts (Figure 4C). The fractional contribution from palmitate oxidation in L-CPT1 expressing hearts, (Figure 4B), were lower than that of both PBS infused hearts and hearts receiving vector containing scrambled DNA (empty). PBS infused controls, control empty virus infusion, and sham aortic banding all resulted in similar $^{13}C$ fractional enrichments of acetyl CoA from [2,4,6,8,10,12,14,16-$^{13}C_8$] palmitate, with mean values ranging from 0.77 to 0.81. The presence of virus alone was insufficient to produce the results observed with L-CPT1 delivery and expression. However, hearts expressing L-CPT1 and hypertrophied hearts displayed strikingly similar values of acetyl CoA $^{13}C$ enrichment, at 0.68 and 0.69, respectively.

### Compensatory increase in glucose oxidation

The reduced palmitate oxidation in hearts expressing L-CPT1 was compensated for by increased glucose oxidation (Figure 5). From combined $^{13}C$ and $^{1}H$ NMR, the oxidation in the TCA cycle of both exogenous $^{13}C$ enriched and endogenous unlabeled ($^{12}C$) glucose to form glutamate was elevated by 60%. No evidence of elevated oxidation of endogenous, myocardial triglyceride stores was apparent, with very similar triglyceride content between L-CPT1 expressing and control hearts: (L-CPT1 = 25.7 ± 5.1 μmol/g dw; PBS = 25.3 ± 5.0). These data demonstrate a compensatory increase in glucose oxidation in response to reduced LCFA oxidation.

### Comparisons to hypertrophy: ANP mRNA with L-CPT1 overexpression

Although palmitate oxidation was reduced in L-CPT1 expressing hearts to the extent of that observed in hypertrophied hearts (Figure 4), which are also known to have elevated L-CPT1 (3), the L-CPT1 expressing hearts showed no evidence of energetic or pathophysiological changes. Hypertrophied hearts have a well-characterized increase in mass and a reduction in bioenergetic state (3,6,28-30). In contrast, heart weight was not elevated in L-CPT1 expressing hearts (L-CPT1 = 2.53 ± 0.07 g; PBS = 2.60 ± 0.08 g), and the phosphocreatine (PCr) to ATP content ratio in these hearts (1.8±0.2), from $^{31}P$ NMR, was not reduced in comparison to PBS controls (1.7±0.1). Also, while hypertrophied myocardium has been reported to display increased anaplerotic flux of three carbon intermediates into the TCA cycle through malic enzyme, the otherwise normal hearts that overexpressed L-CPT1 also displayed normal ratios of anaplerotic to citrate synthase flux: L-CPT1 = 0.052 ± 0.009; PBS = 0.068 ± 0.004. These findings are all consistent with normal contractile work and TCA cycle flux.

Despite these indices of normal myocardial pathology, an unexpected finding was that of significantly elevated ANP message levels, by two-fold in the L-CPT1 overexpressing rat heart (Figure 6). As previously published, mRNA levels of the marker for the hypertrophic response, atrial naturietic peptide (ANP), are elevated in response to pressure overload in the rat heart (3,26). Although the elevation of ANP message was several fold smaller than that observed in hypertrophied hearts following 10 weeks of aortic banding, the finding of elevated ANP expression in hearts acutely expressing L-CPT1 suggests a link between the metabolic activity of the heart, with induced switching to fetal or hypertrophic isoforms of CPT1 and initiation of hypertrophic signaling.

### Acetyl CoA carboxylase, malonyl decarboxylase, and malonyl CoA content

Malonyl CoA, understood to inhibit CPT1 activity, is produced at the outer mitochondrial membrane by acetyl CoA carboxylase 2 (ACC2) via carboxylation of acetyl CoA that is produced from oxidative metabolism. While cytosolic ACC1 has been related to the production of malonyl CoA for LCFA synthesis and elongation, a process not as active in

cardiomyocytes, ACC2 production of malonyl, in concert with malonyl CoA decarboxylase (MCD) action, are understood to work in tandem to regulate malonyl CoA levels.

Interestingly, malonyl CoA content was similar between L-CPT1 expressing and hypertrophied hearts. as with PBS infused shams. The only measurable difference in malonyl CoA was between hypertrophied (HYP) hearts and sham operated hearts (SHAM) with the latter slightly elevated in comparison to all other groups: PBS = 1.54 ± 0.14 nmol/g/ wet tissue wt. (n = 7); L-CPT1 = 1.53 ± 0.09 (n = 13); HYP = 1.43 ± 0.07 (n = 4) ; SHAM = 1.99 ± 0.17 (n = 4), $P<0.05$ vs. HYP.

Phosphorylation of ACC2 reduces activity, and thus total ACC2 content and phosphorylation levels were examined with relation to the reduced LCFA oxidation observed in hearts overexpressing L-CPT1. The content and phosphorylation level of ACC2, along with MCD levels, for hearts overexpressing L-CPT1 is shown in comparison to sham hearts receiving PBS infusion, in Figure 7. Values for ACC2 in L-CPT1 expressing hearts and PBS infused control are normalized to the total content of pyruvate carboxylase (PC), an enzyme shown to not change in response to hypertrophy (3,6). PC levels were also not different between hearts with L-CPT1 overexpression and PBS infused controls (Supplement Material, Online Figure I). While total ACC2 content was unaffected by L-CPT1 overexpression (Figure 7), the level of ACC2 phosphorylated at serine 218 was reduced by 32% in the L-CPT1 expressing hearts (Figure 7). The reduced level of phosphorylation is consistent with less inhibition, and thus a greater capacity for ACC2 to catalyze the production of malonyl CoA from acetyl CoA (31-33). However, as shown in Figure 7 and seen in other heart models and tissues that display changes in LCFA oxidation, malonyl CoA levels were not different between L-CPT1 expressing hearts and sham hearts receiving PBS infusion (34,35). Consistent with theses findings are the similarity in malonyl CoA decarboxylase (MCD) levels in the L-CPT1 expressing hearts and PBS, sham-infused hearts (Figure 7), and thus the regulatory processes that lowered LCFA oxidation with increased L-CPT1 expression are yet to be identified and likely to involve other processes beyond malonyl CoA levels.

Hypertrophied hearts, resulting from transverse aortic constriction, also contained similar levels of total ACC2 as surgical sham hearts (Figure 8). In contrast to L-CPT1 expressing hearts, the hypertrophied hearts displayed elevated ACC2 phosphorylation, though no direct comparison is available between the L-CPT1 expressing and hypertrophied hearts which were assayed separately. Together the findings of ACC2 content and phosphorylation state and malonyl CoA content, are consistent with a previous finding that demonstrated no directional correlation between LCFA oxidation rates and L-CPT1 content, while M-CPT1 content correlated more closely with LCFA oxidation rates (36). Evidence for muscle type-specific sensitivity of CPT1 activity to malonyl CoA levels also exists, and may shed some insight into the current lack of correlation between malonyl CoA content and LCFA oxidation in L-CPT1 expressing hearts (37). The potential for alternative or yet unidentified mechanisms that mediate L-CPT1 activity are considered in the following section.

## DISCUSSION

With these current results, three conditions in the heart are now linked to elevation in the L-isoform of the carnitine palmitoyltransferse I (CPT1) content in comparison to the normal adult myocardium: a developmental condition of higher L-CPT1 content in the fetal heart, a pathological condition of elevated L-CPT1 content in hypertrophied hearts, and the experimental condition, presented here, of acute increases in L-CPT1 content in the other normal, but genetic altered adult rat heart (1-3, 9). Each of these three conditions that produce elevated L-CPT1 in the heart, and thus shift the isoform distribution of CPT1 from

muscle toward liver enzymes, are now associated with reduced fatty acid oxidation and elevated carbohydrate metabolism (3,5,6,11,13,14,38). Indeed, although suggested as an adaptation to maintain LCFA oxidation, L-CPT1 has never been associated with increased LCFA oxidation in cardiomyocytes (2). Importantly, the current study reports on actual rates of palmitate oxidation observed from on-line $^{13}C$ NMR observation of beating hearts that are responding to an acute induction of L-CPT1 expression in the intact functioning heart.

We have previously reported the first observation of increased L-CPT1 protein expression in hypertrophied heats (3). We demonstrated the inefficiency in energy metabolism as a consequence of the shift away from the high yield of ATP provided by long chain fatty acids (LCFA), in the absence of limited oxygen delivery and tissue $PO_2$ as has been shown to be the case in the remodeled and hypertrophied heart (39,40). Recent findings specific to maladpative expression of malic enzyme-1 also indicate inefficient metabolism of carbohydrates in the hypertrophied heart which were not in evidence in the current study of non-pathological hearts with an isolated elevation of L-CTP1 expression (3,6). Thus, the current findings enable focus on the link between L-CPT1 expression in heart and LCFA oxidation, without the many overlaying complexities of the diseased myocardium. Interestingly, as discussed below, L-CPT1 expression induced elevated ANP levels, a marker of the hypertrophic response, suggesting a direct link to the pathogenesis of cardiac hypertrophy.

Elevated expression of L-CPT1 in hypertrophied hearts coincided with a reduced rate of LCFA oxidation (3,6). While the muscle isoform, M-CPT1, is predominant in heart, the liver (L) isoform is upregulated in hypertrophy. Although suggested as an adaptation to maintain LCFA oxidation, LCPT1 has never been associated with increased LCFA oxidation in cardiomyocytes. Interestingly, the hearts studied during brief, acute overexpression of L-CPT1, following cardiac specific introduction of the exogenous gene, also showed evidence of significantly increased glucose oxidation in replacement of lost LCFA oxidation. Triacylglyceride content was not affected by the presence of additional L-CPT1, and with no evidence of increased LCFA contributions from stored TAG was present, a general shift from LCFA to glucose oxidation is evident in supporting the otherwise normal cardiac workload of hearts overexpressing L-CPT1 (Figure 2). Values for the contribution of $^{13}C$ palmitate to acetyl CoA production demonstrate that the presence of L-CPT1 was required to reduce palmitate oxidation and not the introduction of the viral vector, because hearts receiving vector containing the scrambled code (empty) showed control levels of acetyl CoA enrichment from $^{13}C$ palmitate. Thus, the induced expression of L-CPT1 in the intact heart produced a reduction in LCFA oxidation similar to that of hypertrophied hearts, and contrary to the expectation of elevated LCFA oxidation were the reduced sensitivity to malonyl CoA levels and elevated carnitine affinity the sole determinants of L-CPT1 activity in the intact myocardium (1,9,10).

Interestingly, CPT1 activity in tissues containing predominantly L-CPT1 is not directly proportional to protein content, and thus our previous observations in both hypertrophied heart and now the L -CPT1 overexpressing hearts may also reflect this lack of proportionality (3,36). Induced expression of the exogenous LCPT1 gene produced CPT1 protein content changes in the rat heart that were similar to those reported in the hypertrophied rat heart, with a 4-5 fold increase in L-CPT1 protein and minimal change in the level of M-CPT1 protein (3). Thus, the metabolic shifts between LCFA and glucose oxidation reported here correspond to a relative distribution of the liver and muscle isoforms of CPT1 that is representative of the hypertrophied heart. A relatively surprising finding was that of increased levels of a well-known marker of hypertrophic signaling, ANP expression, in hearts overexpressing L-CPT1, which did not occur in sham infused hearts subjected to the same surgical procedure. Although ANP mRNA levels were a great deal higher in hearts

that had been subjected to pressure overload for 10 weeks and displaying pathologic hypertrophy, the L-CPT1 expressing hearts exhibited ANP message levels that were already double those of the sham group within only 72 hours (Figure 6) (3). This finding indicates a provocative link between metabolic regulation at the level of gene expression and induction of hypertrophic signaling pathways in the heart, that are directionally similar to the metabolic phenotype and ANP expression in pathological cardiac hypertrophy.

The findings also suggests the action of alternative regulatory mechanisms for the activation of L-CPT1 versus M-CPT1 in the cardiomyocyte beyond the inhibitory effects of malonyl CoA, that are becoming increasing apparent in metabolic studies of both cardiac muscle and other tissue types (34-37,41). Malonyl CoA content was similar between L-CPT1 expressing and PBS infused hearts, despite clearly reduced LCFA oxidation in hearts overexpressing L-CPT1. Yet, in confirming the well-reported reduction in LCFA oxidation in hypertrophied hearts, the current findings also show malonyl CoA to actually be lower in the hypertrophied hearts with reduced LCFA oxidation, as is consistent with limited acetyl CoA production from LCFA oxidation (41). Nevertheless, malonyl CoA content was similar between L-CPT1 hearts and hypertrophied hearts. The similar malonyl CoA content among these groups is also consistent with similar enzyme protein levels of malonyl decarboxylase and acetyl CoA carboxylase 2 (ACC2) between L-CPT1 hearts and PBS controls, as well as between hypertrophied hearts and surgical shams. The only distinctions appear in the level of ACC2 phosphorylation at serine 218 (P-ACC2), where L-CPT1 hearts displayed lowered P-ACC2 compared to PBS controls and hypertrophied hearts showed elevated P-ACC2 content.

Since phosphorylation inactivates ACC2 for production of malonyl CoA, the reduced P-ACC2 content in L-CPT1 hearts may be consistent with the observed reduction in palmitate oxidation, but not consistent with the unchanged malonyl CoA content when compared to controls. Hypertrophied hearts displayed lower malonyl CoA levels compared to surgical sham hearts, yet P-ACC2 content was higher than in sham operated hearts. If malonyl CoA is the inhibitory agent to affect CPT1, then irrespective of relative P-ACC2 content, the reduced palmitate oxidation in the L-CPT1 hearts and hypertrophied hearts is not related to ACC2 phosphorylation levels. Thus, while the P-ACC2 assay results remain the only data to suggest a differential downstream regulation of L-CPT1 activity between the L-CPT1 hearts and hypertrophied hearts, similarities in malonyl CoA content in L-CPT1 hearts to that of the PBS controls and hypertrophied hearts strongly suggests that other factors besides total tissue malonyl CoA content regulate the observed LCFA oxidation through CPT1. This leads to questions beyond the scope of this one study, regarding the role of ACC1 in the cytosol in contributing to the total malonyl CoA that is measured in such studies.

Recently published reports indicate no direct relationship between increased malonyl CoA content and reduced LCFA oxidation in the heart (34,41,42). While these recent studies demonstrating the absence of a link between malonyl CoA content and LCFA oxidation were performed on hearts with a predominantly normal distribution of M-CPT1 and L-CPT1 contents, the current findings suggest that L-CPT1 may be subject to additional levels of regulation that have yet to be fully identified. Indeed, Kim et al report on a malonyl CoA-resistant level of palmitate oxidation in red versus white skeletal muscle preparations (37). Therefore, in light of the present findings and newly emerging considerations, we can not rule out other factors such as post-translational modifications, invoked in the intact functioning myocardium that limit LCFA oxidation through L-CPT1 beyond malonyl CoA, even though studies indicate this isoform to be less responsive to malonyl CoA than M-CPT1 in culture cell preparations (10).

Beyond the regulation of CPT1 activity as previously described, but not yet well characterized in the intact myocardium, the induction of increased L-CPT1 isoform content in the intact heart produced an anticipated reduction in both the rate of palmitate oxidation and the contribution of palmitate to β-oxidation for the production of tricarboxylic acid cycle intermediates within the energy yielding oxidative pathways of the mitochondria. The shift in isoform distribution between the L and M isoforms present in these hearts, following acute delivery of the exogenous gene for L-CPT1, was similar to the distribution previously reported in the hypertrophied heart. While L-CPT1 expression had no measurable effect on M-CPT1 content, this isoform shift in otherwise normal rat hearts produced a reduction in palmitate oxidation that recapitulated the phenotype of reduced LCFA oxidation in the hypertrophied hearts. Indeed, increased incorporation of isotope from $^{13}C$ enriched glucose into the 4-carbon position of glutamate demonstrated elevated glucose oxidation in L-CPT1 expressing hearts, indicating a shift from LCFA oxidation to glucose oxidation. However, unlike hypertrophied hearts, L-CPT1 hearts did not display a change in the metabolic fate of glycolytic end products, with a shift toward the anaplerotic production of malate, which has been linked, to elevated malic enzyme 1 content in cardiac hypertrophy (3,6). Rather, acute overexpression of L-CPT1 induced a reduction in palmitate oxidation, with a consequential, compensatory shift toward increased glucose oxidation to maintain energy demands.

Nevertheless, the link between L-CPT1 expression and the induction of metabolic remodeling in hypertrophied hearts has been demonstrated here to be a key component of altered LCFA oxidation. Elevated L-CPT1 is associated with provocative elevation of ANP message, a marker of hypertrophic signal induction, in the otherwise non-pathogenic myocardium. The implications of this work are that previous notions of L-CPT1 regulation are incomplete when applied to the intact functioning heart. Indeed, the findings suggest that a single key metabolic shift, such as altered CPT1 isoform expression and distribution, in the transition to decompensation of the pressure overloaded heart can alone induce the shift away from fatty acid oxidation. The consequences of an acute increase in L-CPT1 expression in the rat heart, as observed here, suggest intriguing links between enzyme activity, metabolic flux, and metabolite content, and the induction of signaling pathways. The latter finding of elevated ANP message in response to increased L-CPT1 content implies the need for closer investigation into influences of metabolic signaling on myocardial remodeling.

## DETAILED MATERIALS AND METHODS

### Adenoviral delivery in vivo

Adult rats (male, Sprague Dawley, 400-450 gm) received an *in vivo* intracoronary perfusion of the heart with either adenovirus carrying cDNA for the rat liver isoform of the carnitine palmitoyltransferase I (Adv.cmv.L-CPT1) at $8\times10^{12}$ viral particles/ml PBS, adenovirus carrying scrambled cDNA (empty) at $8\times10^{12}$ vp/ml as a viral delivery control group, or PBS as a sham control. This open-chest cross-clamp technique, performed on anesthetized (i.p. pentobarbital, 50 mg/kg and 1% isoflurane inhalation) intubated rats, has been described in detail in our previous reports (1-3). The adenovirus expresses the liver isoform of the carnitine palmitoyltransferase I gene ($10^{12}$ viral particles/ml PBS) under a CMV promoter.

Use of the viral vector did not influence L-CPT1 expression in the absence of code for L-CPT1. L-CPT1 expression was similar in hearts that were untreated, PBS infused and supplied empty virus (See Online Figure I). As already referenced in the main text for hypertrophied hearts, for studies examining expression of ACC2, assayed relative to pyruvate carboxylase (PC), delivery and expression of exogenous L-CPT1 gene did not alter PC content (Online Figure II).

All vessels to/from the heart were cross-clamped simultaneously, and the heart was retrograde perfused *in vivo* for 7 min with a calcium free Tyrode solution through catheters position in the aortic root (delivery) and right ventricle (efflux). At the time of adenovirus injection, 0.4 ml of AdV.cmv.L-CPT1 was first delivered through the catheter position in the aortic root. This allowed the adenovirus to circulate down the coronary. Next, the efflux catheter positioned in the right ventricle was removed and an additional 0.5 ml/kg of adenovirus (approximately 0.2 ml) was delivered to the aortic root at 300 ± 100 mmHg peak pressure. After 90 seconds, catheters were repositioned in the right and left ventricle, and unsequestered virus was flushed from the heart with Krebs buffer containing calcium (1.5 mM). The heart rate recovered, the cross-clamp was removed, the chest was closed, and the rats recovered.

The gene delivery technique, referenced above, was reported and confirmed earlier by following the delivery and expression of Ad.cmv.LacZ in whole intact non-failing rat heart (1-3).

## Pressure overload hypertrophy

Cardiac hypertrophy from left-ventricular pressure-overload (LVH) was induced by constricting the transverse aorta (hemoclip) of three-week-old male Sprague Dawley rats, as previously described (2,4-6). This banding procedure relies on the natural growth of the animal to produce a gradually increasing degree of aortic constriction. The rats develop a concentric hypertrophy and increased heart-to-body weight ratio, which is associated, in the short term, with improvement in the systolic function of the heart (2,7-9). At 10-12 weeks post-banding, the animals enter a decompensated stage with depressed LVDP and dP/dt. In this model of left ventricular hypertrophy (LVH), no systemic activation of the sympathetic nervous system or of the renin-angiotensin-aldosterone system occurs (7). Consequently, there are no signs of cardiac lesions, peripheral arteritis, myocardial necrosis, or extensive fibrosis. The rats progress to a dilated cardiac hypertrophy with acute end-stage heart failure at 4-6 months post banding. The sham groups (SHM) underwent similar surgery without placement of the aortic-band.

## NMR spectroscopy and tissue chemistry

NMR measurements were performed on intact beating hearts that were situated within a 10 mm broad band NMR probe inside a 9.4 T NMR magnet interfaced to a Bruker 400 MHz AVANCE console. Sequential, proton-decoupled $^{13}C$ NMR spectra were acquired (2 min each) with natural $^{13}C$ abundance correction using previously reported NMR methods (2,10,11). Magnetic field homogeneity was optimized by shimming to a proton line width of 10-20 Hz. Carbon spectra were acquired at 101 MHz with bilevel broad-band decoupling and subtracted from naturally abundant endogenous $^{13}C$ signal. $^{31}P$ spectra were acquired at 161 MHz over 2 minute intervals at the start of each protocol, prior to acquisition of $^{13}C$ enriched $^{13}C$ NMR spectra.

Tissue metabolites were extracted from frozen heart tissue using 7% perchloric acid and neutralized with KOH. Tissue extracts were analyzed spectrophotometrically and flurometically for quantification (4,11,12). Glutamate concentration was determined with glutamate dehydrogenase and diaphorase (Roche L-Glutamic acid colorimetric kit.) α-Ketoglutarate content was measured by coupling glutamate-oxaloacetate transaminase (GOT, Roche) with malate dehydrogenase (MDH, Roche) in the presence of excess L-aspartate. Aspartate concentration was measured by coupling GOT with MDH similar to α-ketoglutarate with the exception of excess α-ketoglutarate. Citrate content was determined with citrate lyase (Roche) and MDH. *In vitro* high-resolution $^{13}C$ NMR spectra of tissue extracts reconstituted I 0.5 mL of $D_2O$ were collected with a 5 mm $^{13}C$ probe (Bruker

Instruments, Billerica, MA). Analysis was performed to determine fractional enrichment of [2-$^{13}$C] acetyl CoA (11,13,14). Isotopic enrichment of glutamate from [1,6-$^{13}C_2$] glucose was determined via $^{13}$C NMR of *in vitro* tissue extracts and the relative contributions of exogenous, $^{13}$C enriched glucose and the unlabeled ($^{12}$C) endogenous pool of glycogen determined via $^{1}$H NMR of alanine enrichment as previously described in detail (6).

### $^{13}$C enrichment kinetics and metabolic flux

A set of nine differential equations describes the concentration history of the $^{13}$C in each metabolite and developed in our laboratory was modified to include the additional, rate-determining components of long chain fatty acid uptake into the mitochondria. With a single 9×1 vector $q$ to represent the fractional enrichment of each compartment as a function of time, the model is described in matrix form as

$$\frac{d}{dt}q = M_{TCA} \cdot q + U_{\text{Acetyl}-CoA}$$

where $M_{TCA}$ is a 9×9 matrix characteristic of the TCA cycle, its elements are determined by the TCA cycle flux ($V_{TCA}$), the interconversion rates between the TCA cycle intermediate and glutamate or aspartate ($F_1$ and $F_2$), the level of anaplerosis (y), and the concentrations of each metabolite. The input vector, $U_{Acetyl\text{-}CoA}$, is governed by the fraction of $^{13}$C enriched acetyl-CoA entering the TCA cycle through citrate synthase ($F_c$). The only non-zero element in $U_{Acetyl\text{-}CoA}$ corresponds to the labeling of the 4-carbon position of citrate since [2-$^{13}$C] acetyl-CoA enters the TCA cycle through citrate synthase to enrich the 4-carbon position of citrate (3, 14-15). The nine differential equation in series are:

$$\begin{aligned}
\frac{d}{dt}CIT4 &= \frac{V_{TCA}}{[CIT]} \cdot (F_c - CIT4)\\
\frac{d}{dt}\alpha KG4 &= \frac{V_{TCA}}{[\alpha KG]} \cdot CIT4 - \frac{V_{TCA}+F_1}{[\alpha KG]} \cdot \alpha KG4 + \frac{F_1}{[\alpha KG]} \cdot GLU4\\
\frac{d}{dt}GLU4 &= \frac{F_1}{[GLU]} \cdot (\alpha KG4 - GLU4)\\
\frac{d}{dt}CIT2 &= \frac{V_{TCA}}{[CIT]} \cdot (OAA2 - CIT2)\\
\frac{d}{dt}\alpha KG2 &= \frac{V_{TCA}}{[\alpha KG]} \cdot CIT2 - \frac{V_{TCA}+F_1}{[\alpha KG]} \cdot \alpha KG2 + \frac{F_1}{[\alpha KG]} \cdot GLU2\\
\frac{d}{dt}GLU2 &= \frac{F_1}{[GLU]} \cdot (\alpha KG2 - GLU2)\\
\frac{d}{dt}MAL2 &= \frac{V_{TCA}}{[MAL]} \cdot \left[\frac{1}{2} \cdot \alpha KG2 + \frac{1}{2} \cdot \alpha KG4 - (1+y) \cdot MAL2\right]\\
\frac{d}{dt}OAA2 &= \frac{V_{TCA}}{[OAA]} \cdot MAL2 - \frac{V_{TCA}+F_2}{[OAA]} \cdot OAA2 + \frac{F_2}{[OAA]} \cdot ASP2\\
\frac{d}{dt}ASP2 &= \frac{F_2}{[ASP]} \cdot (OAA2 - ASP2)
\end{aligned}$$

Where CIT, αKG, GLU, MAL, OAA, and ASP denote the metabolites citrate, α-ketoglutarate, glutamate, malate, oxaloacetate, and aspartate, respectively, with the corresponding number of the $^{13}$C enriched carbon position indicated. Where CIT4 is the fractional enrichment level of $^{13}$C at the 4-carbon position of citrate; (i.e., CIT4=[(4-$^{13}$C)CIT]/[CIT]). The equation describing malate enrichment includes anaplerotic and cataplerotic effects (4, 11, 14-15). $F_1$ and $F_2$ are fluxes for interconversion via both transamination and membrane transport, between α-ketoglutarate and glutamate, and between aspartate and oxaloacetate, respectively. Under the current experimental conditions of limited aspartate and alanine, $F_1 = F_2$ (3,11,14-15).

The rate of palmitate oxidation (R) was calculated, under these precise experimental and isotopic enrichment conditions, as the product of $V_{TCA}$ and acetyl CoA enrichment from $^{13}$C palmitate ($F_c$) divided by 8 to account for the 8 acetyl groups produced from the 16 carbon palmitate ($V_{TCA}$ x $F_c$/8).

## Supplementary Material

Refer to Web version on PubMed Central for supplementary material.

## Acknowledgments

**SOURCES OF FUNDING** Supported by NIH Grants, MERIT Award R37 HL49244 and RO1 HL62702.

## Non-standard Abbreviations

| | |
|---|---|
| **CPT1** | carnitine palmitoyltransferase |
| **Adv** | adenovirus |
| **LCFA** | long chain fatty acids |
| **TCA** | tricarboxylic acid |
| **ACC** | acetyl CoA carboxylase |
| **MCD** | malonyl CoA decarboxylase |

## REFERENCES

1. Weis BC, Esser V, Foster DW, McGarry JD. Rat heart expresses two forms of mitochondrial carnitine palmitoyltransferase I. J Biol Chem. 1994; 269:18712–18715. [PubMed: 8034622]
2. Xia Y, Buja LM, McMillan JB. Change in the expression of heart carnitine palmitoyltransferase I isoforms with electrical stimulation of cultured rat neonatal cardiac myocytes. J Biol Chem. 1996; 271:12082–12087. [PubMed: 8662650]
3. Sorokina N, O'Donnell JM, McKinney RD, Pound KM, Woldegiorgis G, LaNoue KF, Ballal K, Taegtmeyer H, Buttrick PM, Lewandowski ED. Recruitment of compensatory pathways to sustain oxidative flux with reduced CPT1 activity characterizes inefficiency in energy metabolism in hypertrophied hearts. Circulation. 2007; 115:2033–2041. [PubMed: 17404155]
4. Sack MN, Rader TA, Park S, Bastin J, McCune SA, Kelly DP. Fatty acid oxidation enzyme gene expression is downregulated in failing heart. Circulation. 1996; 94:2837–2842. [PubMed: 8941110]
5. Allard MF, Schönekess BO, Henning SL, English DR, Lopaschuk GD. Contribution of oxidative metabolism and glycolysis to ATP production in hypertrophied hearts. Am J Physiol: Heart and Circ Physiol. 1994; 267:H742–H750.
6. Pound KM, Sorokina N, Fasano M, Berkich D, LaNoue KF, O'Donnell JM, Lewandowski ED. Substrate-enzyme competition attenuates upregulated anaplerotic flux through malic enzyme in hypertrophied rat heart and restores triacylglyceride content. Circ Res. 2009; 104:805–812. [PubMed: 19213957]
7. McGarry JD, Brown NF. The mitochondrial carnitine palmitoyltransferase system. Eur J Biochem. 1997; 244:1–14. [PubMed: 9063439]
8. Yu GS, Lu Y, Gulick T. Expression of novel isoforms of carnitine palmitoyltransferase I generated by alternative splicing of the CPT-Ib gene. Biochem J. 1998; 334:225–231. [PubMed: 9693124]
9. Brown NF, Weis BC, Husti JE, Foster DW, McGarry JD. Mitochondrial carnitine palmitoyltransferase I isoform switching in the developing rat heart. J Biol Chem. 1995; 270:8952–8957. [PubMed: 7721804]
10. McMillan JB, Wang D, Witters LA, Buja LM. Kinetic properties of carnitine palmitoyltransferase I in cultured neonatal rat cardiac myocytes. Arch Biochem Biophys. 1995; 312:375–384.
11. Makinde AO, Gamble J, Lopaschuk GD. Upregulation of 5′-AMP-activated protein kinase is responsible for the increase in myocardial fatty acid oxidation rates following birth in the newborn rabbit. Circ Res. 1997; 80:482–489. [PubMed: 9118478]
12. Razeghi P, Young ME, Alcorn JL, Moravec CS, Frazier OH, Taegtmeyer H. Metabolic gene expression in fetal and failing human heart. Circulation. 2001; 104:2923–2931. [PubMed: 11739307]

13. Makinde AO, Kantor PF, Lopaschuk GD. Maturation of fatty acid and carbohydrate metabolism in the newborn heart. Mol Cell Biochem. 1998; 188:49–56. [PubMed: 9823010]
14. Lopaschuk GD, Spafford MA, Marsh DR. Glycolysis is the predominant source of myocardial ATP production immediately after birth. Am J Physiol: Heart and Circ Physiol. 1991; 261:H1698–H1705.
15. O'Donnell JM, Lewandowski ED. Efficient, cardiac-specific adenoviral gene transfer in rat heart by isolated retrograde perfusion *in vivo*. Gene Therapy. 2005; 12:958–964. [PubMed: 15789062]
16. O'Donnell JM, Fields A, Xu X, Chowdhury SA, Geenen DL, Bi J. Limited functional and metabolic improvements in hypertrophic and healthy rat heart overexpressing the skeletal muscle isoform of SERCA1 by adenoviral gene transfer *in vivo*. Am J Physiol: Heart Circ Physiol. 2008; 295:H2483–2494. [PubMed: 18952713]
17. O'Donnell JM, Alpert NM, White LT, Lewandowski ED. Coupling of Mitochondrial Fatty Acid Uptake to Oxidative Flux in the Intact Heart. Biophys J. 2002; 82:11–18. [PubMed: 11751291]
18. Lewandowski ED, Yu X, White LT, Doumen C, LaNoue KF, O'Donnell JM. Altered metabolite exchange between subcellular compartments in intact postischemic hearts. Circ Res. 1997; 81:165–174. [PubMed: 9242177]
19. O'Donnell JM, Doumen C, LaNoue KF, White LT, Yu X, Alpert NM, Lewandowski ED. Dehydrogenase regulation of metabolite oxidation and efflux from mitochondria of intact hearts. Am J Physio: Heart and Circ Physiol. 1998; 274:H467–H476.
20. Williamson, JR.; Corkey, BE. Assays of intermediates of the citric acid cycle and related compounds by flourometric enzyme analysis. In: Lowenstein, JM., editor. Methods Enzymol. Academic Press, Inc.; New York: 1967. p. 434-512.
21. Bergmeyer, HU. Methods in enzymatic analysis. Verlag-Chemie International; Deerfield Beach, FL: 1974. p. 2308
22. Sambandam N, Steinmetz M, Chu A, Altarejos JY, Dyck JR, Lopaschuk GD. Malonyl-CoA decarboxylase (MCD) is differentially regulated in subcellular compartments by 5′AMP-activated protein kinase (AMPK). Studies using H9c2 cells overexpressing MCD and AMPK by adenoviral gene transfer technique. Eur J Biochem. 2004; 271:2831–2840. [PubMed: 15206948]
23. Corkey BE. Analysis of acyl-coenzyme A esters in biological samples. Methods Enzymol. 1988; 166:55–70. [PubMed: 3241570]
24. Malloy CR, Sherry AD, Jeffrey FMH. Evaluation of carbon flux and substrate selection through alternate pathways involving the citric acid cycle of the heart by 13C NMR spectroscopy. J Biol Chem. 1988; 265:6964–6971. [PubMed: 3284880]
25. O'Donnell JM, Fields AD, Sorokina N, Lewandowski ED. Absence of endogenous lipid oxidation in heart failure exposes limitations for triacylglycerol storage and turnover. J Mol Cell Cardiol. 2008; 44:315–322. [PubMed: 18155232]
26. Roman BB, Geenen GI, Leitges M, Buttrick PM. PKC-beta is not necessary for cardiac hypertrophy. Am J Physiol: Heart Circ Physiol. 2001; 280:H2264–2270. [PubMed: 11299230]
27. Keung W, Cadete VJ, Palaniyappan A, Jablonski A, Fischer M, Lopaschuk GD. Intracerebroventricular leptin administration differentially alters cardiac energy metabolism in mice fed a low-fat and high-fat diet. J Cardiovasc Pharmacol. 2011; 57:103–113. [PubMed: 20980918]
28. Zhang J, Merkle H, Hendrich K, Garwood M, From AH, Ugurbil K, Bache RJ. Bioenergetic abnormalities associated with severe left ventricular hypertrophy. J Clin Invest. 1993; 92:993–1003. [PubMed: 8349829]
29. Tian R, Nascimben L, Ingwall JS, Lorell BH. Failure to maintain a low ADP concentration impairs diastolic function in hypertrophied rat hearts. Circulation. 1997; 96:1313–1319. [PubMed: 9286964]
30. Ingwall JS. Energy metabolism in heart failure and remodeling. Cardiovasc Res. 2009; 81:412–419. [PubMed: 18987051]
31. Saddik M, Gamble J, Witters LA, Lopaschuk GD. Acetyl-CoA carboxylase regulation of fatty acid oxidation in the heart. J Biol Chem. 1993; 268:25836–25845. [PubMed: 7902355]

32. Lopaschuk GD, Witters LA, Itoi T, Barr R, Barr A. Acetyl-CoA carboxylase involvement in the rapid maturation of fatty acid oxidation in the newborn rabbit heart. J Biol Chem. 1994; 268:25871–25878. [PubMed: 7929291]
33. Dyck JR, Barr AJ, Barr RL, Kolattukudy PE, Lopaschuk GD. Characterization of cardiac malonyl-CoA decarboxylase and its putative role in regulating fatty acid oxidation. Am J Physiol: Heart and Circ Physiol. 1998; 275:H2122–H2129.
34. Zhou L, Huang H, Yuan CL, Keung W, Lopaschuk GD, Stanley WC. Metabolic response to an acute jump in cardiac workload: effects on malonyl-CoA, mechanical efficiency, and fatty acid oxidation. Am J Physiol: Heart Circ Physiol. 2008; 294:H954–H960. [PubMed: 18083904]
35. Lauzier B, Merlen C, Vaillant F, McDuff J, Bouchard B, Beguin PC, Dolinsky VW, Foisy S, Villeneuve LR, Labarthe F, Dyck JR, Allen BG, Charron G, Des Rosiers C. Post-translational modifications, a key process in CD36 function: lessons from the spontaneously hypertensive rat heart. J Mol Cell Cardiol. 2011; 5:99–108. [PubMed: 21510957]
36. Doh KO, Kim YW, Park SY, Lee SK, Park JS, Kim JY. Interrelation between long-chain fatty acid oxidation rate and carnitine palmitoyltransferase 1 activity with different isoforms in rat tissues. Life Sci. 2005; 77:435–443. [PubMed: 15894012]
37. Kim JY, Koves TR, Yu GS, Gulick T, Cortright RN, Dohm GL, Muoio DM. Evidence of a malonyl-CoA-insensitive carnitine palmitoyltransferase I activity in red skeletal muscle. Am J Physiol: Endocrinol Metab. 2002; 282:E1014–E1022. [PubMed: 11934665]
38. Nascimben L, Ingwall JS, Lorell BH, Pinz I, Schultz V, Tornheim K, Tian R. Mechanisms for increased glycolysis in the hypertrophied rat heart. Hypertension. 2004; 44:662–667. [PubMed: 15466668]
39. Bache RJ, Zhang J, Murakami Y, Zhang Y, Cho YK, Merkle H, Gong G, From AH, Ugurbil K. Myocardial oxygenation at high workstates in hearts with left ventricular hypertrophy. Cardiovasc Res. 1999; 42(3):616–626. [PubMed: 10533601]
40. Murakami Y, Zhang Y, Cho YK, Mansoor AM, Chung JK, Chu C, Francis G, Ugurbil K, Bache RJ, From AHL, Jerosch-Herold M, Wilke N, Zhang J. Myocardial oxygenation during high workstates in hearts with postinfarction remodeling. Circulation. 1999; 99:942–948. [PubMed: 10027819]
41. Kudej RK, Fasano M, Zhao X, Lopaschuk GD, Fischer SK, Vatner DE, Vatner SF, Lewandowski ED. Second window of preconditioning normalizes palmitate use for oxidation and improves function during low-flow ischaemia. Cardiovasc Res. 2011; 92:394–400. [PubMed: 21835931]
42. van der Vusse GJ. The fascinating and elusive life of cardiac fatty acids. Cardiovasc Res. 2011; 92:363–364. [PubMed: 21926105]

## Novelty and Significance

**What Is Known?**

- Long chain fatty acids are the preferred fuel for mitochondrial ATP synthesis in the heart, but hypertrophied and failing hearts, like fetal hearts, display a metabolic phenotype of reduced long chain fatty acid oxidation.
- The rate-limiting step of long chain fatty acid (LCFA) oxidation is determined by transport of LCFA into the mitochondria via carnitine palmitoyltransferase I (CPT1) which exists in two isoforms: the adult muscle M-CPT1 that predominates in cardiomyocytes and the liver L-CPT1 which is more highly expressed in the fetal heart.
- Hypertrophied and failing hearts express higher than normal levels of the liver, L, isoform as do fetal hearts in comparison to normal adult hearts.

**What New Information Does This Article Contribute?**

- Acute overexpression of L-CPT1 in otherwise normal rat hearts, via cardiac-specific delivery of an exogenous gene, decreased LCFA oxidation.
- LCFA oxidation was reduced in hearts expressing L-CPT1, suggesting other factors influence L-CPT1 activity in intact, functioning hearts.
- Increased expression of L-CPT1 and lower rate of LCFA oxidation in normal hearts were associated with increases in a marker of cardiac hypertrophy, atrial natriuretic peptide (ANP).

This study challenges dogma regarding the role of CPT1, in cardiac hypertrophy. Our previous work indicates that the reversion to a fetal gene program in cardiac hypertrophy increased myocardial content of the fetal form of CPT1, the L isoform, co-expressed with adult M-CPT1. Mimicking the hypertrophic isoform distribution of CPT1, in non-pathogenic hearts, recapitulated the lower LCFA oxidation rates that occur with cardiac hypertrophy. Importantly, the induced metabolic change elevated ANP These findings provide novel insights into the complex interrelationship of metabolic gene expression, regulation of LCFA oxidation, and the induction of the hypertrophic response.

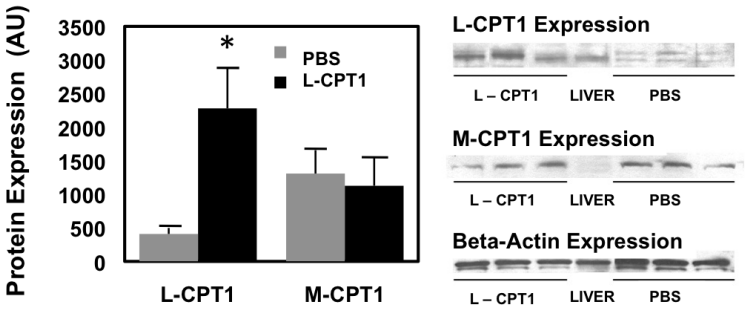


**Figure 1. Expression levels of L-CPT1 at 72 hours in hearts receiving intracoronary Adv.CPT1L, versus PBS-infused sham hearts (PBS)**

Protein levels for liver (L) and muscle (M) isoforms of CPT1 are normalized to beta-actin and expressed in arbitrary units (AU). Rat liver (LIV) was used as a positive control of L-CPT1 expression. L-CPT1 protein was elevated in hearts receiving delivery of exogenous gene, with no apparent effects on M-CPT1 content. Gray bar, PBS. Black Bar, L-CPT1. *, $P<0.05$ versus PBS group.

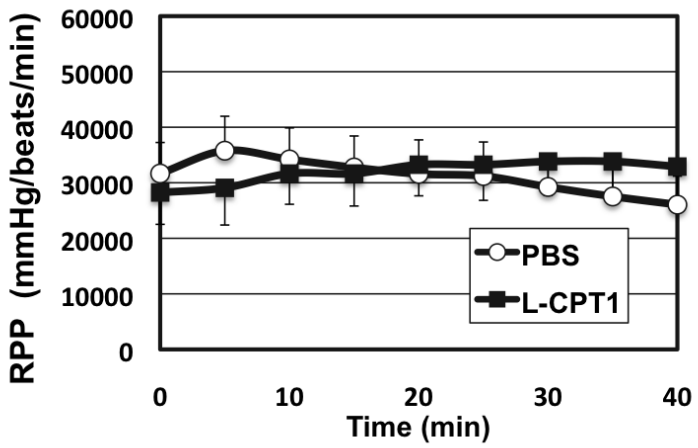


**Figure 2. Similar workloads in isolated perfused rats following delivery of exogenous L-CPT1 gene or PBS infusion 72 hours post infusion**

Values are rate-pressure-product over course of heart perfusion during collection of $^{13}C$ NMR data. Open circle, PBS. Closed square, L-CPT1.

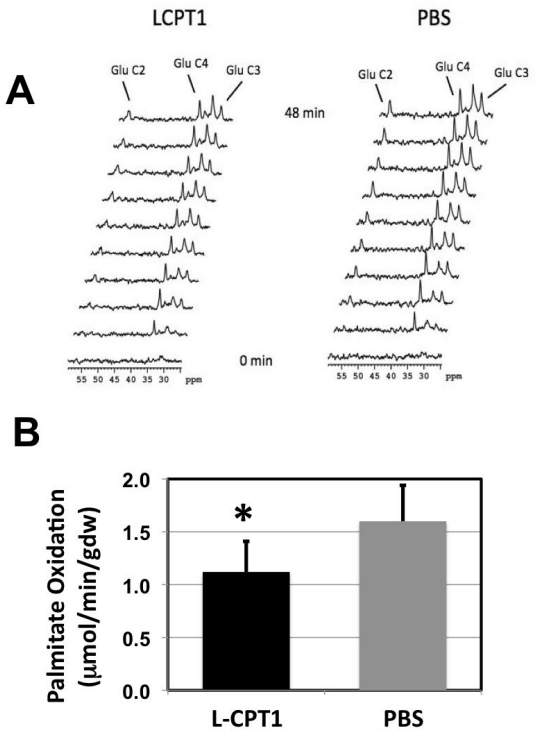


**Figure 3. Oxidation rates with $^{13}$C palmitate from sequential $^{13}$C NMR spectra of isolated perfused hearts**

**A.** Representative, selected spectra acquired in 2 minute intervals showing sequential enrichment of glutamate carbons as a consequence of [2,4,6,8,10,12,14,16-$^{13}C_8$] palmitate oxidation in isolated perfused rats hearts. NMR spectra display progressive enrichment over perfusion protocol (from bottom to top). At left is a data set of $^{13}$C spectra from a single heart overexpressing L-CPT1 and at right is a set of sequential $^{13}$C spectra from a control heart infused with PBS **B.** Palmitate oxidation was reduced in hearts overexpressing L-CPT1 (black bar) compared to that of PBS controls (gray bar). *, P<0.05 versus PBS.

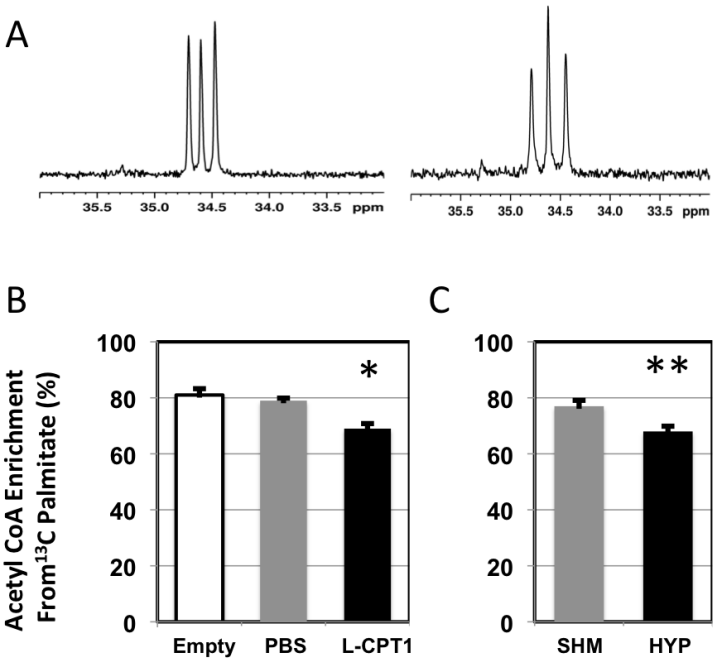


**Figure 4. Reduced contribution of $^{13}$C palmitate to actyl CoA in mitochondria of L-CPT1 expressing hearts and hypertrophied hearts from high resolution, *in vitro* $^{13}$C NMR spectra of tissue extract displaying glutamate isotopomer distribution**

**A.** Expanded region of the glutamate 4-carbon $^{13}$C resonance signal within NMR spectrum displaying distinct differences in multiple structures between a PBS control heart (left) and a heart overexpressing L-CPT1 (right). Note prominent central singlet and reduced doublet structure of resonance from L-CPT1 heart corresponding to lower contribution of $^{13}$C palmitate to oxidative metabolism. **B.** Reduced acetyl CoA enrichment from $^{13}$C palmitate in hearts overexpressing L-CPT1 (black bar) compared to heart receiving PBS (gray bar) or virus containing nonsense code (Empty, white bar). *, $P<0.05$ versus Empty and PBS groups. **C**. Reduced acetyl CoA enrichment from $^{13}$C palmitate in hypertrophied hearts (HYP, black bar) compared to sham operated hearts (SHM, gray bar). **, $P<0.05$ versus SHM. Note similarity of reduced values between L-CPT1 (B) and HYP groups (C).

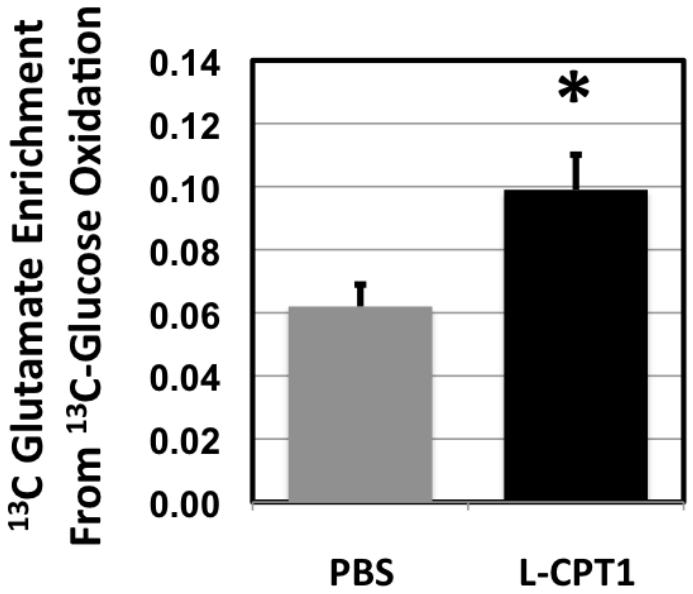


**Figure 5.**
Elevated oxidation of $^{13}$C glucose in the presence of unlabeled palmitate in hearts expressing L-CPT1 (black bar). Note increased glutamate enrichment at the 4-carbon of L-CPT1 over PBS control (gray bar). *, P<0.05 versus PBS.

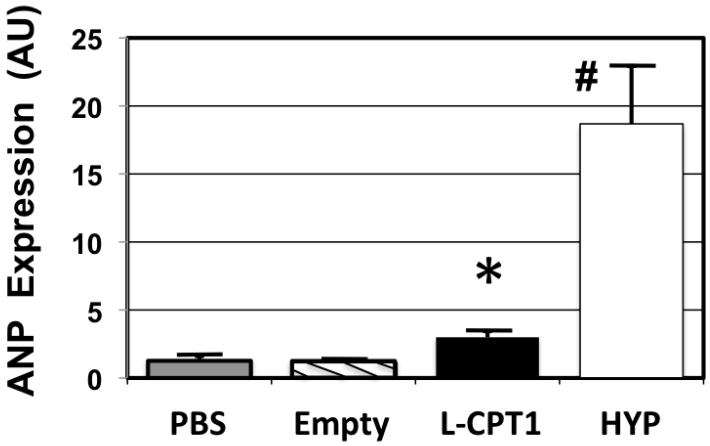


**Figure 6. Atrial natriuretic peptide (ANP) mRNA content was elevated in L-CPT1 expressing hearts (black bar) and hypertrophied hearts (HYP, 10 weeks aortic banding, white bar)**

Empty virus had no affect on ANP content compared to PBS infusion. *, P<0.05 versus PBS and HYP; #, P<0.05 versus PBS and L-CPT1.

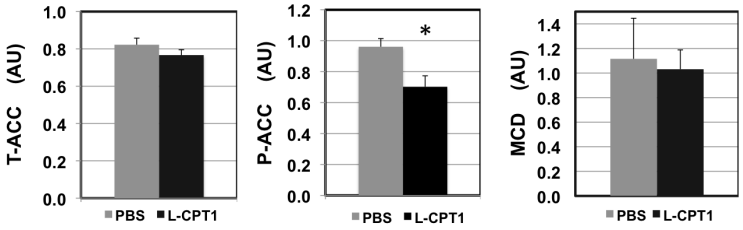


**Figure 7. Protein content of total acetyl CoA carboxylase 2 (T-ACC), phosphorylated (Ser 218) ACC2 (P-ACC), and malonyl decarboxylase (MCD) in PBS control heart (gray bars) and L-CPT1 expressing hearts (black bars)**

All values shown as arbitrary units (AU) normalized to pyruvate carboxylase protein. Note reduced levels of P-ACC in L-CPT1. *, $P<0.05$ versus PBS.

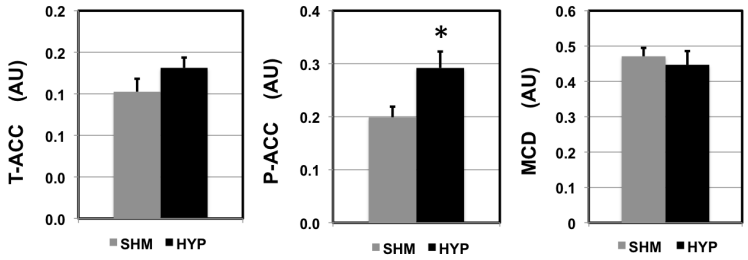


**Figure 8. Protein content of total acetyl CoA carboxylase 2 (T-ACC), phosphorylated (ser 218) ACC2 (P-ACC), and malonyl decarboxylase (MCD) in sham operated hearts (SHM, gray bars) and hypertrophied hearts (HYP, 10 weeks aortic banding, black bars)**

All values shown as arbitrary units (AU) normalized to glyceraldehyde dehydrogenase protein. Note elevated levels of P-ACC in HYP. *, P<0.05 versus SHM.